Development/Plasticity/Repair

Distinct Transcriptomes Define Rostral and Caudal Serotonin Neurons

Christi J. Wylie,[1] **Timothy J. Hendricks,**[3] **Bing Zhang,**[4] **Lily Wang,**[5] **Pengcheng Lu,**[4] **Patrick Leahy,**[2] **Stephanie Fox,**[1] **Hiroshi Maeno,**[1] **and Evan S. Deneris**[1]

[1]Department of Neurosciences and [2]Case Comprehensive Cancer Center, Case Western Reserve University, Cleveland, Ohio 44106, [3]Molecular Neurobiology Laboratory, Salk Institute for Biological Studies, La Jolla, California 92037, and Departments of [4]Biomedical Informatics and [5]Biostatistics, Vanderbilt University School of Medicine, Nashville, Tennessee 37232

The molecular architecture of developing serotonin (5HT) neurons is poorly understood, yet its determination is likely to be essential for elucidating functional heterogeneity of these cells and the contribution of serotonergic dysfunction to disease pathogenesis. Here, we describe the purification of postmitotic embryonic 5HT neurons by flow cytometry for whole-genome microarray expression profiling of this unitary monoaminergic neuron type. Our studies identified significantly enriched expression of hundreds of unique genes in 5HT neurons, thus providing an abundance of new serotonergic markers. Furthermore, we identified several hundred transcripts encoding homeodomain, axon guidance, cell adhesion, intracellular signaling, ion transport, and imprinted genes associated with various neuro-developmental disorders that were differentially enriched in developing rostral and caudal 5HT neurons. These findings suggested a homeodomain code that distinguishes rostral and caudal 5HT neurons. Indeed, verification studies demonstrated that Hmx homeodomain and Hox gene expression defined an Hmx$^+$ rostral subtype and Hox$^+$ caudal subtype. Expression of engrailed genes in a subset of 5HT neurons in the rostral domain further distinguished two subtypes defined as Hmx$^+$En$^+$ and Hmx$^+$En$^-$. The differential enrichment of gene sets for different canonical pathways and gene ontology categories provided additional evidence for heterogeneity between rostral and caudal 5HT neurons. These findings demonstrate a deep transcriptome and biological pathway duality for neurons that give rise to the ascending and descending serotonergic subsystems. Our databases provide a rich, clinically relevant resource for definition of 5HT neuron subtypes and elucidation of the genetic networks required for serotonergic function.

Introduction

Genetic perturbation of embryonic brain serotonin (5HT) neuron gene expression causes developmental alterations in numerous rodent behaviors (Hendricks et al., 2003; Hodges et al., 2008; Lerch-Haner et al., 2008) and is thought to significantly contribute to susceptibility of human emotional and stress-related neurodevelopmental pathogenesis in adulthood (Ansorge et al., 2007). Evidence in support of these ideas is primarily derived from the study of genes encoding the rate-limiting biosynthetic enzyme tryptophan hydroxylase 2 (TPH2), the 5HT transporter (Sert), and the serotonin 1a autoreceptor (Leonardo and Hen, 2006; Holmes, 2008; Le François et al., 2008). As these proteins operate in complex networks of poorly defined cellular regulatory pathways (Prasad et al., 2005), many other genes are likely to be important for serotonergic function, and many of them may be relevant to human mental disease pathogenesis. Yet their iden-

tity is largely obscure in part because of a lack of an approach to isolate 5HT neurons for comprehensive gene expression profiling of this CNS cell type.

Gene expression profiles of 5HT neurons may be complex despite their common monoaminergic character if, as is evident, these cells are heterogeneous. 5HT neurons can be distinguished according to their axonal trajectories and physiological properties (Beck et al., 2004; Kocsis et al., 2006). Rostral 5HT neurons, born anterior to rhombomere 4 (r4) give rise to ascending axonal projections, which modulate circuitry needed for emotional responses, circadian rhythms, and energy balance (Lucki, 1998; Sodhi and Sanders-Bush, 2004). A caudal cluster, posterior to r4 gives rise to descending pathways, which modulate a diversity of physiological processes including cardiorespiratory homeostasis, thermoregulation, and nociception (Mason, 2001; Erickson et al., 2007; Zhao et al., 2007; Gargaglioni et al., 2008; Hodges et al., 2008). Differences in progenitor identities (Jacob et al., 2007; Lillesaar et al., 2007), extrinsic signaling dependencies (Ye et al., 1998), transcription factor requirements (Hendricks et al., 2003), and distinct rhombomere-specific neuron sublineages (Jensen et al., 2008) suggest complexity in rostrocaudal serotonergic differentiation programs that generate these cells. These potentially distinct programs may direct different patterns of 5HT neuron gene expression and account for the diversity of behaviors and physiological processes under serotonergic modulation as well as the large number of neuropsychiatric disorders in which sero-

Figure 1. ePet-EYFP expression marks rostral and caudal 5HT neurons in the embryonic ventral hindbrain. **A**, Whole-mount view of an ePet-EYFP transgenic brain at E14.5. Both rostral and caudal 5HT neuronal cell bodies and axonal projections were brightly marked by EYFP fluorescence. **A′**, High-magnification view (8×) of caudal 5HT axonal projections to the spinal cord. **B–D**, Tiled confocal *z*-stack images of 5HT immunoreactivity (red) and EYFP fluorescence at E12.5 (**B**, sagittal view) and at E14.5 in the caudal (**C**, sagittal view) and rostral (**D**, coronal view) domains. Scale bars: **B**, 100 μm; **C, D**, 200 μm.

nergic dysfunction has been implicated (Holmes, 2008). Few genetic markers distinguish differentiated 5HT neurons, however, and therefore their molecular differences are poorly defined.

Whole-genome profiling is a powerful approach for analysis of molecular complexity in CNS neuronal and glia cell types and the developmental programs specifying their diversity (Sugino et al., 2006; Cahoy et al., 2008). Here, we report a purification protocol for enrichment of embryonic postmitotic 5HT neurons followed by microarray analysis of 5HT neuron gene expression profiles. Our microarray, verification, and bioinformatics studies identify several hundred genes and many biological pathways whose expression distinguishes rostral and caudal 5HT neurons. Our transcriptome datasets provide an abundance of new markers to enable molecular classification of 5HT neuron subtypes and a rich resource for identification of new serotonergic genes of potential relevance to mental disease pathogenesis.

Materials and Methods

Transgenic mice. ePet-EYFP mice were generated in a C57/SJL background. Embryos were genotyped either by PCR with primers 5′-GAA CTC CAG CAG GAC CAT GT-3′ and 5′-TAT ATC ATG GCC GAC AAG CA-3′ or by a fluorescence dissecting microscope.

Dissection of ePet-EYFP$^+$ neural tubes. Pregnant mice [embryonic day 0.5 (E0.5) defined as the morning of plug formation] were killed by cervical dislocation in accordance with Institutional Animal Care and Use Committee regulations. E12.5 embryos were removed from uteri into ice-cold L15 media (Invitrogen). Hindbrains were dissected and visualized under an inverted fluorescent dissecting microscope to identify ePet-EYFP$^+$ transgenics. A nontransgenic embryo was identified and processed simultaneously as a negative control to gate for background fluorescence on the cell sorter. Hindbrains were dissected into rostral and caudal

regions using the absence of YFP fluorescence in rhombomere 4 as a landmark. Specifically, the neural tube was isolated from the mesencephalic flexure to the spinal cord and cut at the pontine flexure to separate rostral and caudal hindbrain regions (see Fig. 2*A*).

Cell dissociation. Rostral and caudal hindbrains were enzymatically digested in 1× trypsin-EDTA (Invitrogen) diluted in Ca^{2+}/Mg^{2+}-free DPBS (Invitrogen) at 37°C for 17 min. Tissues were washed three times in ice-cold Leibovitz L15 media (Invitrogen). Samples were resuspended in L15 containing 0.1% BSA (Invitrogen) and 0.1 μg/ml DNase (Sigma) and then mechanically dissociated by gentle trituration with a fire-polished glass pipette to create a single-cell suspension. Cells were pelleted and resuspended in L15 containing 0.1% BSA.

Flow cytometry. Cells were passed through a 40 μm filter and immediately sorted on a Becton Dickinson FACS Aria digital cell sorter equipped with an argon laser providing excitation of 200 mW at 488 nm. YFP fluorescence was detected with the standard FL2 filter set (560 nm dichroic, 585/42 nm bandpass). Sort pressure was 35 psi with an 85 μm nozzle tip driven at 39.5 kHz. Maximum event rate was conservatively limited to 5000/s. Forward scatter height versus width gating was used to eliminate aggregates. YFP fluorescent cells were identified by characteristic red versus orange fluorescence and were sorted directly into tubes containing Trizol (Invitrogen) for subsequent RNA extraction or into L15 media for confirmation of sort purity. A typical sort with 4–5 transgenic embryos at E12.5 yielded ~45,000 rostral YFP$^+$ and 30,000 caudal YFP$^+$ 5HT neurons. Using this protocol, we collected ~200,000 cells for each of the four cell groups to be profiled: R$^+$ (rostral YFP$^+$), R$^-$ (rostral YFP$^-$), C$^+$ (caudal YFP$^+$), and C$^-$ (caudal YFP$^-$).

RNA isolation, amplification, and microarray hybridization. Total RNA was isolated after the addition of tRNA as carrier and RNA quality was inspected with a Bioanalyser 2100 (Agilent). One-round amplification was performed using the MessageAmp II Kit (Ambion). *In vitro* transcription with biotin incorporation (Bioarray High Yield RNA Transcript Labeling, Enzo) was used to generate cRNA probes. The quantity of cRNA was measured by Nanodrop 1000 (Nanodrop Technologies). Ten micrograms of cRNA for each cell type were fragmented and hybridized overnight at 42°C to Affymetrix whole-genome arrays (Mouse Genome 430 2.0). Each Affymetrix 430 2.0 array contains 45,037 oligonucleotide probe sets, which represent 20,832 unique genes. After hybridization, the chips underwent stringency washes in a Genechip Fluidics Station (Affymetrix) and were scanned at high resolution (Affymetrix High Density GeneChip Scanner 3000). Three biological replicates from different litters, independent FACS isolation, amplification, and hybridization were performed to assess reproducibility. DAT files were later used to generate CEL files. Affymetrix GCOS using MAS 5.0 statistical algorithms was used to convert CEL files into Excel spread sheets. Standard quality assessment procedures were performed for all hybridizations according to Affymetrix recommendations.

Microarray data processing. Present/Absent calls for each probe set were calculated with Affymetrix MAS 5.0 package of Bioconductor (Reimers and Carey, 2006). Default parameters were used for the calculation. CEL files from 12 chips were normalized using the Robust MultiChip Averaging (RMA) algorithm as implemented in Bioconductor (Reimers and Carey, 2006).

Multiple-group comparison and hierarchical clustering. The ANOVA test in the Limma package (Smyth, 2005) was used to identify probe sets

that were differentially expressed across the four test groups. The p values generated from the ANOVA test were further adjusted using the Benjamini and Hochberg correction (Benjamini and Hochberg, 1995). In this comparison, differentially expressed probe sets were selected based on two criteria: (1) adjusted p values <0.001, and (2) at least a twofold change between the groups with highest and lowest average expression values. Hierarchical clustering analysis (Eisen et al., 1998) was then applied to the selected probe sets. Average linkage was used in the clustering analysis with Pearson's correlation coefficient as the similarity measurement.

Pairwise comparisons. For pairwise comparisons, the t test in the Limma package was used to identify differentially expressed probe sets between the two groups under comparison. The implementation of t test in Limma uses an empirical Bayes method to moderate the SEs of the estimated log-fold changes. This results in more stable inference and improved power, especially for experiments with small number of arrays. The p values generated from the t test were further adjusted using the Benjamini and Hochberg correction (Benjamini and Hochberg, 1995) to account for multiple comparisons. An adjusted p value of 0.01 (i.e., 1% false discovery rate) was used to select differentially expressed probe sets.

Knowledge-guided gene set-level analysis. We used the mixed models approach (Wang et al., 2008) to assess coordinated changes of genes at the gene set level in serotonin neurons. Gene sets derived from the Gene Ontology (GO) were downloaded from the Molecular Signatures Database (MSigDB) (http://www.broad. mit.edu/gsea/msigdb/index. jsp). For each gene set, this approach compares the average gene expression levels of the two groups (e.g., serotonin neurons vs nonserotonin neurons) for gene sets versus other genes while controlling for correlations between genes. Mixed models analysis uses continuous evidence from each gene so that the results do not depend on any significance cutoff for single genes as in conventional overrepresentation analysis. It was shown to have more favorable statistical properties compared to traditional gene set analysis methods (Wang et al., 2008). Because many gene sets were examined, to control for the rate of false-positive findings by chance, we adjusted nominal p values using Bonferroni correction.

Double-label in situ hybridization/immunohistochemistry. DIG-labeled antisense probes were synthesized with digoxigenin-11-UTP according to the manufacturer's instructions (Roche). Tissues were fixed with 4% paraformaldehyde overnight and then cryoprotected in 30% sucrose. Ten to twenty micrometer cryostat sections were collected on Superfrost Plus slides (Fisher). Sections were fixed again for 5 min, washed three times with 1× PBS, treated with proteinase K (1 μg/ml) for 3 min, washed three times with 1× PBS, acetylated in 0.35% (v/v) acetic anhydride at room temperature in 100 mM triethanolamine pH 8.0 for 10 min, and then rinsed three times in 1× PBS. Sections were prehybridized for 1 h at room temperature in hybridization buffer (50% deionized formamide, 5× SSC, 5× Denhardt's solution, 250 μg/ml Baker's yeast tRNA, 500 μg/ml salmon sperm DNA). Probe was diluted 1:100 in hybridization buffer and applied to slides, which were then sealed with Hybrislip coverslips (Grace Biolabs). Hybridization was performed overnight at 65–68°C. The next day coverslips were removed in 5× SSC. Sections were then washed for 2 h in 0.2× SSC at 65–68°C. Sections were
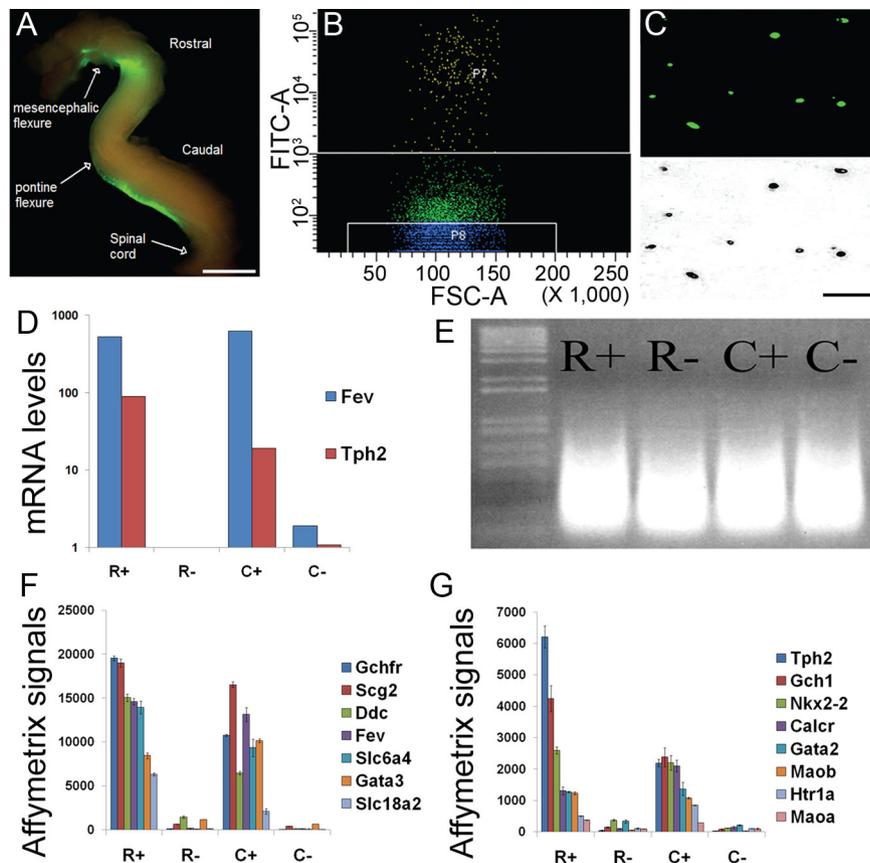
Figure 2. Purification and expression profiling of rostral and caudal 5HT neurons. **A**, E12.5 ePet-EYFP neural tubes were dissected and incisions made at the mesencephalic flexure, pontine flexure, and spinal cord to separate the rostral and caudal domains. **B**, Single-cell suspensions of rostral and caudal neural tubes were subjected to FACS. EYFP$^+$ cells were collected in gate P7 (top) and nonfluorescent cells were collected in gate P8 (bottom). The fluorescent and nonfluorescent fractions were separated by one log unit to ensure pure populations for gene expression profiling. **C**, Sorting efficiency was verified by examining purified cells under fluorescence (top) and phase-contrast (bottom) microscopy. **D**, RNA was isolated from rostral YFP$^+$ (R$^+$), rostral YFP$^-$ (R$^-$), caudal YFP$^+$ (C$^+$), and caudal YFP$^-$ (C$^-$) sorted cells and then assayed by Taqman RT-PCR for two known 5HT neuron-specific genes, Fev and Tph2. **E**, Total RNA from 200,000 sorted cells each for rostral 5HT YFP$^+$ (R$^+$), rostral non-5HT (R$^-$), caudal 5HT YFP$^+$ (C$^+$), and caudal non-5HT (C$^-$) was used for one round of amplification to generate cRNA probes. **F, G**, Enriched expression of well established highly expressed (**F**) and more moderately expressed (**G**) markers of 5HT neurons were detected in R$^+$ and C$^+$ neurons by microarray hybridization. The y-axis equals the gene expression level determined by MAS 5.0. Error bars represent SEM. Scale bars: **A**, **C**, 100 μm.

then equilibrated in 1× B1 (100 mM Tris, pH 7.4, 150 mM NaCl) for 10 min, blocked for 1 h in 10% heat-inactivated goat serum diluted in B1, and then incubated overnight at 4°C with sheep anti-DIG-alkaline phosphatase-conjugated Fab fragments (Roche) diluted 1:5000 in blocking buffer. The next day slides were washed 3 × 15 min in 1× B1, equilibrated in freshly prepared B2 (300 mM Tris, pH 9.5, 300 mM NaCl, 150 mM MgCl₂) for 10 min, and then developed in chromogen solution containing 340 μg/ml NBT, 180 μg/ml BCIP, and 240 μg/ml levamisole (all Sigma) in B2 at room temperature for 2–16 h. For double labeling, slides were washed 3 × 5 min in 1× PBS, blocked 1 h in 10% goat serum in 1× PBST, and incubated with anti-rabbit GFP (Clontech) at 1:1000 overnight at 4°C. Sections were then washed 3 × 5 min in 1× PBS and incubated with a 1:1000 dilution of biotinylated goat anti-rabbit IgG antibody for 2 h at room temperature. Horseradish peroxidase staining was performed using the avidin–biotin–peroxidase complex (Vectastain ABC kit, Vector Laboratories) and SigmaFast DAB tablets (Sigma). Sections were dehydrated through graded ethanols and xylene and coverslipped with DPX (Electron Microscopy Sciences).

Immunohistochemistry and antibodies. Immunohistochemistry was performed on 20 μm cryostat sections from embryos that were fixed in 4% PFA for 1–2 h and then cryoprotected in 30% sucrose. Pan-engrailed antiserum was a gift from Alexandra Joyner (Sloan-Kettering Institute). Hox antibodies were a gift from Thomas Jessell (Columbia University

Medical Center). Pan-Meis antibody was a gift from Steve O'Gorman (Case Western Reserve University). Dilutions were 1:8000 for rabbit anti-HoxA3, 1:5000 for rabbit anti-HoxC4, 1:1000 for rabbit anti-pan-Meis, and 1:100 for rabbit anti-pan-engrailed antibodies. Goat anti-rabbit Texas Red secondary antibody (Jackson ImmunoResearch Laboratories) was used at 1:400.

Confocal microscopy. Twenty to thirty micrometer sections were imaged on a Zeiss LSM 510 Meta confocal microscope. For z-stacks, images were collected every 2–3 μm and compressed using Zeiss LSM Image software.

Taqman quantitative real-time reverse transcription-PCR. Total RNA was extracted from FACS-isolated cells according to the Trizol method (Invitrogen). R^+, R^-, C^+, and C^- RNA samples were delivered to the Gene Expression and Genotyping Facility at Case Western Reserve. Samples were then converted to cDNA and then assayed by Taqman (Applied Biosystems) in triplicate for candidate gene confirmation. The C_T (cycle number at threshold) was used to calculate the relative amounts of mRNA molecules for a given gene. The C_T of each target gene was normalized by subtracting the C_T value of the housekeeping gene β-actin, which gave the value ΔC_T. The difference in the ΔC_T from the cell type of interest and a control cell type gave $\Delta\Delta C_T$. The relative quantitative change was shown as $2^{-\Delta\Delta C_T}$. Taqman assay IDs for each gene are as follows: Fev, Mm00462220_n1; Tph2, Mm00557717_m1; Rnf112 (Zfp179), Mm008396908_g1; Zcchc12, Mm00511603_m1; Tox, Mm00455231_m1; 2010204K13RIK, Mm01971390_s1; AW551984, Mm00724626_m1; 1700042O10RIK, Mm01191108_m1; Hmx2, Mm01165724_m1; Hmx3, Mm00433957_g1; Pou3f1, Mm00843534_s1; En1, Mm00438709_m1; En2, Mm00438710_m1; HoxA3, Mm01326402_m1; HoxB3, Mm00650701_m1; HoxD3, Mm00439371_m1; HoxA4, Mm01335255_g1; HoxB4, Mm00957964_m1; HoxC4, Mm00442838_m1; HoxA5, Mm00439362_m1; HoxB5, Mm00657672_m1; HoxC5, Mm00433971_m1.

Results

Purification and gene expression profiling of embryonic rostral and caudal 5HT neurons

The ePet-EYFP transgenic mouse line expresses enhanced yellow fluorescent protein (EYFP) specifically in adult 5HT neurons (Scott et al., 2005). To determine whether this line would be suitable for identification and purification of embryonic 5HT neurons we determined the pattern of EYFP expression in the developing hindbrain. Both rostral and caudal embryonic 5HT neurons and their axons could be readily visualized by expression of YFP in the ePet-EYFP line (Fig. 1 and data not shown). YFP was colocalized with 5HT immunoreactivity but was not detected elsewhere in the hindbrain (Fig. 1 *B–D* and data not shown) consistent with endogenous Pet-1 expression (Hendricks et al., 1999). As expected, there was an absence of EYFP fluorescence in rhombomere 4 where 5HT neurons are not generated (Fig. 1*A*). Thus, the embryonic expression pattern of the ePet-EYFP line indicated that it could be used for identification and purification by flow cytometry of differentiating 5HT neurons from the rostral and caudal hindbrain.

We chose to profile gene expression at E12.5 when 5HT neurons are actively differentiating and cell migration and axon pathfinding are underway. At this developmental stage virtually all rostral 5HT neurons have differentiated (Pattyn et al., 2003). However, in the caudal hindbrain 5HT neuron differentiation is not yet complete at E12.5 and therefore the serotonergic cells at this stage are a mixture of postmitotic precursors and mature 5HT neurons. Rostral and caudal hindbrain domains were dissected from E12.5 ePet-EYFP embryos (Fig. 2*A*), dissociated with trypsin digestion and triturated in preparation for flow cytometry. For each sort (Fig. 2*B*), we also collected rostral YFP^- (R^-) and caudal YFP^- (C^-) reference cells, which comprise primarily neighboring hindbrain motoneurons and interneurons. The purity of sorted R^+ and C^+ neurons was analyzed by examining a
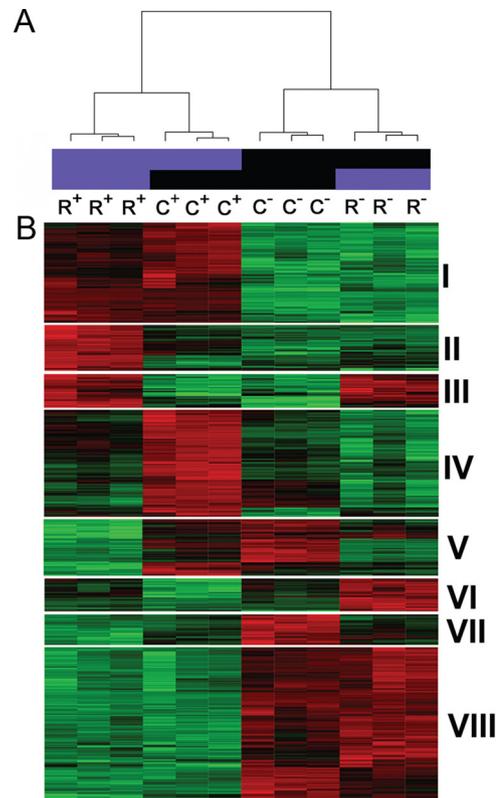
Figure 3. Unsupervised hierarchical clustering of serotonergic gene expression. *A*, Dendrogram showing unsupervised hierarchical clustering of R^+, C^+, R^-, and C^- gene expression profiles from the 12 arrays. Biological replicates show a high degree of reproducibility. *B*, Heat map displays eight distinct clusters of enriched gene expression in R^+, C^+, R^-, and C^- cell populations at E12.5. Each row represents the relative levels of expression for a single gene. The red or green color indicates high or low expression, respectively. Each column shows the expression profile for a single biological sample. Cluster I, Enriched gene expression in rostral 5HT and caudal 5HT neurons (R^+C^+); cluster II, enriched gene expression in rostral 5HT neurons (R^+); cluster III, enriched gene expression in rostral 5HT and rostral non-5HT neurons (R^+R^-); cluster IV, enriched gene expression in caudal 5HT neurons (C^+); cluster V, enriched gene expression in caudal 5HT and caudal non-5HT neurons (C^+C^-); cluster VI, enriched gene expression in rostral non-5HT neurons (R^-); cluster VII, enriched gene expression in caudal non-5HT neurons (C^-); and cluster VIII, enriched gene expression in rostral and caudal non-5HT neurons (R^-C^-).

portion of the cells under fluorescence and phase contrast microscopy to determine the number of cells that were also YFP^+ (Fig. 2*C*). Approximately 98% of rostral and caudal cells were YFP^+ using our sorting parameters. We confirmed the purity of our sorted 5HT neurons by assaying for the expression of Fev (Pet-1) and Tph2, two genes whose expression in the CNS is restricted to 5HT neurons. Taqman real-time reverse transcription (RT)-PCR analyses of R^+, C^+, R^-, and C^- total RNAs showed at least a 10-fold enrichment of Fev and Tph2 in R^+ and C^+ relative to R^- and C^- (Fig. 2*D*).

Probes (Fig. 2*E*) were generated from 200,000 sorted rostral and caudal YFP^+ cells and hybridized to Affymetrix 430 2.0 arrays. These hybridizations were used to generate present/absent (P/A) calls as described in the Materials and Methods. An annotated master list of expression signals and P/A calls for all 12 array profiles is presented in Dataset 1 (available at www.jneurosci.org as supplemental material). The data discussed in this publication have been deposited in the NCBI Gene Expression Omnibus (GEO) and are accessible through GEO Series accession number GSE19474 (http://www.ncbi.nlm.nih.gov/geo/query/acc.cgi?acc= GSE19474). We first analyzed our dataset to confirm that known

Table 1. Top 50 genes with enriched expression in R^+C^+ 5HT neurons (cluster I)

Affy ID	Fold change	Gene symbol	Gene title
1430105_at	19.9	1700042O10Rik	RIKEN cDNA 1700042O10 gene
1433434_at, 1433435_at	18.6, 7.1	AW551984	Expressed sequence AW551984
1460303_at, 1421867_at	14.8, 5.3	Nr3c1	Nuclear receptor subfamily 3, group C, member 1
1427038_at	10.9	Penk1	Preproenkephalin 1
1445546_at	10.8	AI844685	Expressed sequence AI844685
1445247_at	9.9	C530044C16Rik	RIKEN cDNA C530044C16 gene
1460578_at	9.6	Fgd5	FYVE, RhoGEF, and PH domain-containing 5
1421498_a_at	9.4	2010204K13Rik	RIKEN cDNA 2010204K13 gene
1433578_at	8.9	EG545758	Predicted gene, EG545758/solute carrier family 10 (sodium/bile acid cotransporter family), member 4
1436004_at	8.7	Usp27x	Ubiquitin-specific peptidase 27, X chromosome
1456108_x_at, 1418360_at, 1418360_at	8.5, 4.7, 4.2	Rnf112	Ring finger protein 112
1440891_at, 1435722_at	8.2, 6.2	Gria4	Glutamate receptor, ionotropic, AMPA4 (α4)
1458230_at	7.1	—	—
1450344_a_at	7.0	Ptger3	Prostaglandin E receptor 3 (subtype EP3)
1441330_at	6.9	Crb1	Crumbs homolog 1 (*Drosophila*)
1436772_at	6.7	—	—
1424842_a_at	6.6	Arhgap24	Rho GTPase-activating protein 24
1455416_at	6.1	C130021I20Rik	Riken cDNA C130021I20 gene
1420955_at	5.9	Vsnl1	Visinin-like 1
1452981_at, 1449563_at	5.8, 5.1	Cntn1	Contactin 1
1441729_at	5.6	—	—
1456712_at, 1455260_at	5.5, 4.4	Lcorl	Ligand-dependent nuclear receptor corepressor-like
1447707_s_at, 1452202_at	5.4, 3.9	Pde2a	Phosphodiesterase 2A, cGMP-stimulated
1460097_at	5.3	—	—
1428434_at	5.2	Zcchc12	Zinc finger, CCHC domain-containing 12
1447669_s_at	5.2	Gng4	Guanine nucleotide-binding protein (G-protein), γ4
1435939_s_at	5.1	Hepacam2	HEPACAM family member 2
1417441_at	5.1	Dnajc12	DnaJ (Hsp40) homolog, subfamily C, member 12
1447946_at	4.9	Adam23	A disintegrin and metallopeptidase domain 23
1441625_at	4.9	Rimbp2	RIMS-binding protein 2
1428599_at	4.8	Kndc1	Kinase noncatalytic C-lobe domain (KIND)-containing 1
1456783_at	4.7	Zdbf2	Zinc finger, DBF-type-containing 2
1434800_at	4.7	Sv2b	Synaptic vesicle glycoprotein 2 b
1441055_at	4.4	Akap2/Palm2	A kinase (PRKA) anchor protein 2/paralemmin 2/Palm2-Akap2 protein
1419200_at	4.3	Fxyd7	FXYD domain-containing ion transport regulator 7
1433884_at	4.3	Syt1	Synaptotagmin I
1416762_at, 1456642_x_at	4.3, 4.0	S100a10	S100 calcium-binding protein A10 (calpactin)
1433643_at	4.2	Cacna2d1	Calcium channel, voltage-dependent, α2/δ subunit 1
1429702_at	4.1	2900072G11Rik	RIKEN cDNA 2900072G11 gene
1426622_a_at	4.0	Qpct	Glutaminyl-peptide cyclotransferase (glutaminyl cyclase)
1442077_at	4.0	2310076G05Rik	RIKEN cDNA 2310076G05 gene
1433582_at	3.9	1190002N15Rik	RIKEN cDNA 1190002N15 gene/hypothetical protein LOC100044725
1451046_at	3.9	LOC100047651	Similar to FOG/zinc finger protein, multitype 1
1417398_at, 1448689_at	3.8, 3.6	Rras2	Related RAS viral (r-ras) oncogene homolog 2
1452114_s_at	3.7	Igfbp5	Insulin-like growth factor-binding protein 5
1433919_at	3.7	Asb4	Ankyrin repeat and SOCS box-containing 4
1452936_at	3.7	Crtac1	Cartilage acidic protein 1
1428221_at	3.7	Klhdc8b	Kelch domain-containing 8B
1417411_at	3.6	Nap1l5	Nucleosome assembly protein 1-like 5
1447933_at	3.5	Kif26a	Kinesin family member 26A

serotonergic genes were reproducibly detected. The arrays confirmed the enriched expression of 15 known serotonergic genes in R^+ and C^+ relative to R^- and C^- (Fig. 2*F,G*). Average signal intensities for these known 5HT neuron expressed genes ranged from 15,154 for probe set, 1435750_at, representing the GTP cyclohydrolase feedback regulator (Gchfr) to 335 for one of the probe sets, 1442676_at, that represents monoamine oxidase A (MaoA). We note, however, that our array studies failed to detect expression of some genes known to be expressed in 5HT neurons such as those encoding the htr1b receptor and α1b adrenergic receptor. The reason for these discrepancies is unclear but may reflect immature levels of expression at E12.5. Nevertheless, the detection of the majority of the traditional 5HT neuron markers

further indicates that the process of hindbrain dissociation and flow cytometry did not result in qualitative changes in the phenotype of these purified cells and therefore supports strong confidence in our approach for discovery of serotonergic gene expression.

We next analyzed the array data to assemble 5HT neuron gene expression profiles. 5HT neuron development and function depends on the activity of broadly expressed genes such as housekeeping genes as well as genes whose expression is highly selective for 5HT neurons such as Fev or TPH2. Thus, our first goal was to assemble a list of all genes expressed in E12.5 5HT neurons without consideration of their possible enrichment in R^+ and C^+ cell groups. We based our conservative estimate of the number of
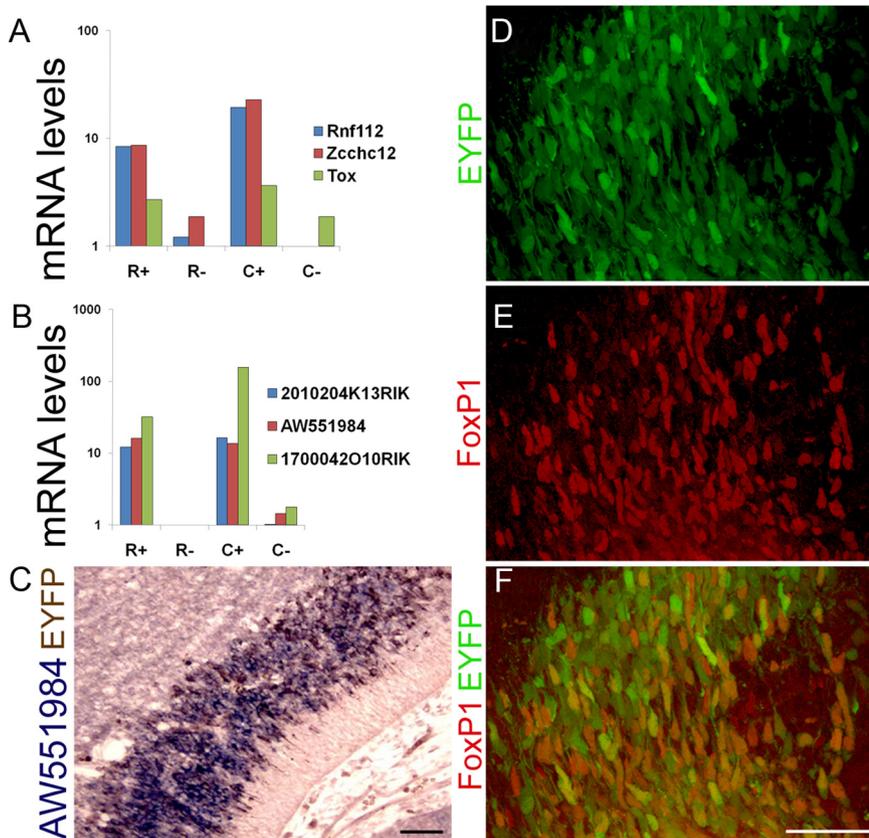
Figure 4. Verification of 5HT neuron-enriched gene expression. ***A***, ***B***, Taqman RT-PCR verified 5HT neuron-enriched expression of transcription factors Rnf112, Zcchc12, Tox and RIKEN genes 2010204K13Rik, AW551984, and 1700042O10Rik. ***C***, Double-label immunohistochemistry for EYFP (brown) and *in situ* hybridization for AW551984 transcript (purple) verified the enriched expression of est AW551984 in 5HT neurons. ***D–F***, Coimmunohistochemical staining of E12.5 neural tube confirmed FoxP1 (***E***) expression in YFP$^+$ (***D***) 5HT neurons (***F***, overlay). Scale bars: ***C***, 40 μm; ***D–F***, 100 μm.

complex innervation patterns of serotonergic axons that initiate around E12.5 led us to search for genes encoding axon pathfinding/cell adhesion molecules and 191 such genes were identified as expressed in R$^+$ and C$^+$ (supplemental Table S3, available at www.jneurosci.org as supplemental material). Finally, the neurochemically rich afferent input to 5HT neurons and the prominent role of the 5HT system in maintenance of homeostatic states prompted a search for genes encoding ion transport proteins, receptors and kinases. These searches uncovered 65 ion channel genes (supplemental Table S4, available at www.jneurosci.org as supplemental material), 118 solute carrier genes (supplemental Table S5, available at www. jneurosci.org as supplemental material), 38 G-protein-coupled receptors (supplemental Table S6, available at www.jneurosci.org as supplemental material), and 175 unique kinases (supplemental Table S7, available at www.jneurosci.org as supplemental material) expressed in R$^+$ and C$^+$.

5HT neuron-enriched gene expression

We next sought to determine differentially expressed genes in our four groups of profiled cell populations. Using the ANOVA test, we found 1806 probe sets that were differentially expressed across the four groups based on the criteria described in the Material and Methods. Unsupervised hierarchical clustering was applied to reveal clusters of biological samples and clusters of genes with similar expression patterns (Fig. 3). As shown in the dendrogram in Figure 3A, two distinct sample clusters were identified that correspond to the serotonergic and nonserotonergic cell groups we examined. Interestingly, the six serotonergic profiles sorted into two subclusters that correspond to the rostrocaudal origins of serotonin neurons, thus providing the first clear indication of large gene expression differences in rostral and caudal serotonin neurons. Not surprisingly, however, rostral and caudal serotonin neurons were more similar to each other than to nonserotonergic neurons from the same rostrocaudal level, while profiles of rostral and caudal nonserotonergic neurons were more similar to each other than to those of serotonergic neurons. Biological replicates for each of the different cell groups showed the highest similarities in gene expression patterns, thus further demonstrating the high reproducibility of our overall profiling method.

Hierarchical clustering of the genes revealed eight distinct gene expression clusters (I–VIII) that segregated according to serotonergic identity and rostrocaudal positions (Fig. 3B). Clusters I–V comprise unique profiles of ~800 transcripts differentially enriched in R$^+$ and C$^+$ serotonin neurons, while clusters VI–VIII comprise transcripts enriched in R$^-$ and C$^-$ nonserotonergic reference cell populations.

We systematically examined each of the five serotonergic clusters to identify prominent molecular features of 5HT neuron transcriptomes. Cluster I is comprised of 317 probe sets corresponding to 274 unique transcripts enriched in both rostral

unique genes expressed in E12.5 5HT neurons on the number of probe sets in Dataset 1 (available at www.jneurosci.org as supplemental material) whose expression was reproducibly detected at a selected minimum threshold signal intensity level. Expression of a probe set was considered reproducibly detected if it was scored as present (P) in all three biological replicates of R$^+$ or C$^+$ profiles. The threshold signal intensity was set to the level of signal intensity for monoamine oxidase A probe set 1442676_at, whose mean expression level (335) was lowest of all probe sets for known serotonergic genes (Fig. 2G). Using these criteria, we estimated 12,559 probe sets were expressed in R$^+$C$^+$ cells, which corresponds to 8186 individual genes, 866 RIKEN cDNAs and 435 ESTs. A database of E12.5 5HT neuron expressed genes with respective mean signal intensity levels in R$^+$ and C$^+$ is available in Dataset 2 (available at www.jneurosci.org as supplemental material). A search of the Allen Institute Brain Atlas (Ng et al., 2009) revealed 250 genes with a TPH2-like expression pattern in the adult brain (supplemental Table S1, available at www.jneurosci. org as supplemental material). We detected expression of 155 of these genes in R$^+$ and C$^+$, indicating that many but not all TPH2-like genes initiate expression during embryogenesis.

A major aim of this study was to identify new potential transcriptional determinants of 5HT neuron development. Therefore, we searched our list of 5HT neuron expressed genes according to protein molecular function and identified >800 genes encoding DNA binding proteins (supplemental Table S2, available at www.jneurosci.org as supplemental material). The

Table 2. Gene ontology and pathway enrichment in R^+C^+ 5HT neurons

Code	Gene set name	Size	R^+ Bon	C^+ Bon
Biological process-enriched gene sets				
310	Lipid metabolic process	195/271	0.002807	8.72×10^{-6}
125	Ceramide metabolic process	7/10	0.011107	0.003837
62	Calcium ion transport	12/24	0.017271	2.07×10^{-5}
765	Sphingolipid metabolic process	12/24	0.041981	0.0021
573	Proteolysis	78/162	1.87×10^{-5}	3.94×10^{-9}
561	Protein processing	19/42	0.03184	0.01963
335	Membrane lipid metabolic process	36/88	0.008563	0.000265
246	G-protein-coupled receptor protein signaling pathway	101/290	0.000209	0.003268
557	Protein modification process	214/567	2.02×10^{-7}	5.86×10^{-6}
456	Peptide metabolic process	5/9	7.1×10^{-6}	0.682079
763	Sphingoid metabolic process	9/11	0.055297	0.015825
168	Di-, trivalent inorganic cation transport	17/29	0.152911	0.000429
86	Cellular lipid metabolic process	116/212	0.05149	0.001441
338	Metal ion transport	53/102	1	0.00036
74	Cation transport	62/128	0.138503	7.68×10^{-5}
555	Protein metabolic process	514/1066	0.134745	0.000225
296	Ion transport	75/161	1	0.001533
Cellular component-enriched gene sets				
232	Voltage-gated calcium channel complex	12/15	1.49×10^{-5}	0.04144
103	Intrinsic to membrane	387/1169	2.76×10^{-11}	3.1×10^{-13}
92	Integral to plasma membrane	275/846	2.79×10^{-5}	7.08×10^{-6}
193	Protein complex	176/703	6.86×10^{-7}	1.28×10^{-6}
Molecular function-enriched gene sets				
393	Voltage-gated channel activity	32/66	0.000161	5.47×10^{-6}
102	Exopeptidase activity	13/28	0.001926	5.75×10^{-5}
30	ATPase activity coupled to transmembrane movement of ions	10/22	0.041303	0.03688
159	Ion channel activity	57/126	0.000252	7.01×10^{-9}
160	Ion transmembrane transporter activity	94/245	0.011539	2.22×10^{-7}
50	Carboxypeptidase activity	4/12	0.033525	0.041814
201	Neuropeptide hormone activity	5/10	0.016866	1
18	Aminopeptidase activity	9/10	1	0.000943
314	Serine-type peptidase activity	26/41	0.277263	2.87×10^{-5}
312	Serine-type endopeptidase activity	22/37	0.889975	8.5×10^{-5}
55	Cation transmembrane transporter activity	100/194	0.053817	3.06×10^{-6}
Canonical pathway-enriched gene sets				
509	RAB pathway	9/10	6.33×10^{-7}	0.000801
454	Nos1 pathway	15/20	0.001063	0.00845
249	HSA00600 sphingolipid metabolism	18/31	0.00138	0.022235
244	HSA00564 glycerophospholipid metabolism	32/68	0.002839	0.000696

Bon, Bonferroni-corrected p value.

and caudal 5HT neurons (supplemental Table S8, available at www.jneurosci.org as supplemental material). Only 13 of these genes have been shown by the Allen Institute to have a TPH2-like expression pattern in the adult brain. Further filtering of the cluster I list to exclude additional known serotonergic genes revealed 250 new genes with severalfold enrichment in R^+ and C^+ cells, thus validating our approach for discovery of 5HT neuron gene expression in the developing hindbrain (Table 1). Several of these potential new markers of developing 5HT neurons have well defined functions in other neural and non-neural cell types, while the function of others have not been elucidated.

Because of our interest in genes controlling 5HT neuron development, we focused our enrichment verification studies primarily on genes encoding known and putative transcriptional regulators. The genes we selected for confirmation spanned the full range of probe set signal intensities (1350 – 15,000) (supplemental Table S8, available at www.jneurosci.org as supplemental material). Taqman RT-PCR (Fig. 4A) confirmed the highly enriched expression of the zinc finger factor, Zcchc12, which is also known as Smad-interacting zinc finger protein (Sizn1) and whose known sequence variants are associated with mental retar-

dation (Cho et al., 2008b). Zcchc12 is an X-linked gene that has been shown to promote cholinergic transmitter phenotype by stimulating bone morphogenetic protein-dependent regulation of choline acetyltransferase and vesicular acetylcholine transporter genes in basal forebrain cholinergic neurons (Cho et al., 2008a). These known functions raise the possibility that Zcchc12 also regulates serotonergic neuron neurochemical properties. Rnf112 (also known as Zfp179 or Znf179) is thought to encode a zinc finger transcription factor (Seki et al., 1999). We verified Rnf112 enrichment in rostral and caudal 5HT neurons by Taqman RT-PCR (Fig. 4A). The Rnf112 gene maps within the common chromosomal 17p11.2 duplicated region that is responsible for Potocki–Lupski syndrome (PLS) (Kimura et al., 1997). This syndrome is characterized by neurodevelopmental and behavioral phenotypes including anxiety and autism spectrum features (Potocki et al., 2007). We confirmed expression of some other genes exhibiting more modest enrichment in R^+ and C^+. For example, Tox (thymocyte selection-associated high mobility group box) is a gene required for T-cell maturation and is also strongly expressed in the developing cingulate and motor cortex of the E16 mouse brain (Mühlfriedel et al., 2007). We found a

Table 3. Top genes with enriched expression in R $^+$ (cluster II) and R $^+$R $^-$ (cluster III)

Affy ID	Fold change	Gene symbol	Gene title
R $^+$-enriched genes			
1425804_at	29.7	Hmx2	H6 homeobox 2
1420444_at	27.1	Slc22a3	Solute carrier family 22 (organic cation transporter), member 3
1437339_s_at, 1451406_a_at	8.9, 6.1	Pcsk5	Proprotein convertase subtilisin/kexin type 5
1449031_at	8.3	Cited1	Cbp/p300-interacting transactivator with Glu/Asp-rich C-terminal domain 1
1452065_at	7.9	Vstm2a	V-set and transmembrane domain-containing 2A
1456512_at	7.2	Pdzrn4	PDZ domain-containing RING finger 4
1425083_at	6.8	Otor	Otoraplin
1422052_at, 1455365_at	5.7, 4.8	Cdh8	Cadherin 8
1450047_at	5.3	Hs6st2	Heparan sulfate 6-O-sulfotransferase 2
1419719_at	5.1	Gabrb1	GABA$_A$ receptor, subunit β 1
1426621_a_at	4.9	Ppp2r2b	Protein phosphatase 2 (formerly 2A), regulatory subunit B (PR 52), β isoform
1436662_at	4.5	Sorcs1	VPS10 domain receptor protein SORCS 1
1436137_at	4.3	Slc6a17	Solute carrier family 6 (neurotransmitter transporter), member 17
1440545_at	4.2	ENSMUSG00000075319	Predicted gene, ENSMUSG00000075319
1440455_at, 1456609_at	4.0, 3.6	Camk2n1	Calcium/calmodulin-dependent protein kinase II inhibitor 1
1452728_at	3.9	Kirrel3	Kin of IRRE-like 3 (*Drosophila*)
1422150_at	3.8	Hmx3	H6 homeobox 3
1431569_a_at	3.8	Lypd1	Ly6/Plaur domain-containing 1
1426712_at	3.8	Slc6a15	Solute carrier family 6 (neurotransmitter transporter), member 15
1423551_at, 1434115_at	3.8, 3.3	Cdh13	Cadherin 13
1456778_at	3.7	—	—
1449979_a_at	3.6	Spock3	Sparc/osteonectin, cwcv, and kazal-like domains proteoglycan 3
1440425_at	3.6	—	—
1429390_at	3.5	Acpl2	Acid phosphatase-like 2
1459214_at	3.4	—	—
1438729_at	3.4	Sox1	SRY-box-containing gene 1
R $^+$R $^-$-enriched genes			
1418868_at	18.3	En2	Engrailed 2
1438009_at	11.1	Hist1h2ab/Hist1h2ac	Histone cluster 1
1437996_s_at, 1455471_at	8.4, 6.6	00012D20Rik	RIKEN cDNA 1500012D20 gene
1418618_at	7.2	En1	Engrailed 1
1418666_at	4.5	Ptx3	Pentraxin-related gene
1456127_at	4.5	Cnpy1	Canopy 1 homolog (zebrafish)
1455620_at	3.6	EG628779	Predicted gene, EG628779
1442558_at	3.4	ENSMUSG00000072792	Predicted gene, ENSMUSG00000072792
1451888_a_at	3.0	Odz4	Odd Oz/ten-m homolog 4 (*Drosophila*)
1447676_x_at, 1425560_a_at	2.8, 2.7	S100a16	S100 calcium-binding protein A16
1454178_at	2.6	2610027F03Rik	RIKEN cDNA 2610027F03 gene
1434458_at	2.5	Fst	Follistatin
1452968_at	2.4	Cthrc1	Collagen triple helix repeat-containing 1
1451983_at	2.2	Irx1	Iroquois-related homeobox 1 (*Drosophila*)
1427252_at	2.1	Dmrtb1	DMRT-like family B with proline-rich C-terminal, 1
1439557_s_at	2.1	Ldb2	LIM domain-binding 2
1435917_at	1.9	Ociad2	OCIA domain-containing 2
1426298_at	1.9	Irx2/LOC100045612	Iroquois-related homeobox 2 (*Drosophila*)
1436449_at	1.8	—	—
1451479_a_at	1.8	Tmem53	Transmembrane protein 53
1435297_at	1.8	Gjd2	Gap junction protein, δ 2
1425530_a_at	1.7	Stx3	Syntaxin 3
1418502_a_at	1.7	Oxr1	Oxidation resistance 1
1424133_at	1.5	Tmem98	Transmembrane protein 98

3.0-fold enrichment of Tox expression in R $^+$ and C $^+$ by array analysis and a similar level of enrichment was also detected by Taqman assays (Fig. 4A). RIKEN cDNA 1700042O10RIK, showed a 20-fold enrichment in R $^+$C $^+$ by array detection and 30-fold and 150-fold enrichment in R $^+$ and C $^+$, respectively, by Taqman RT-PCR (Fig. 4B). Interestingly, 1700042O10RIK encodes a noncoding RNA of unknown function whose gene is embedded in the dopa decarboxylase gene but on opposite strands. This finding raises the intriguing hypothesis that 1700042O10RIK RNA is a novel regulator of ddc transcription in 5HT neurons by a *cis*-antisense mechanism. We also verified ex-

pression of other genes whose functions cannot be predicted by homology comparisons. RIKEN cDNA 2010204K13RIK encodes a predicted single transmembrane 83 amino acid protein and was enriched 10-fold in both R $^+$ and C $^+$. In addition, we confirmed the strong expression of EST AW551984 by both Taqman RT-PCR (Fig. 4B) and double-label *in situ* hybridization (Fig. 4C). Confirmation of the 5HT neuron-specific expression of these uncharacterized protein-coding genes suggests novel proteins carry out functions specifically in 5HT neurons. FoxP1, a forkhead domain transcription factor, is required for motoneuron diversity and ultimately the development of spinal cord motor
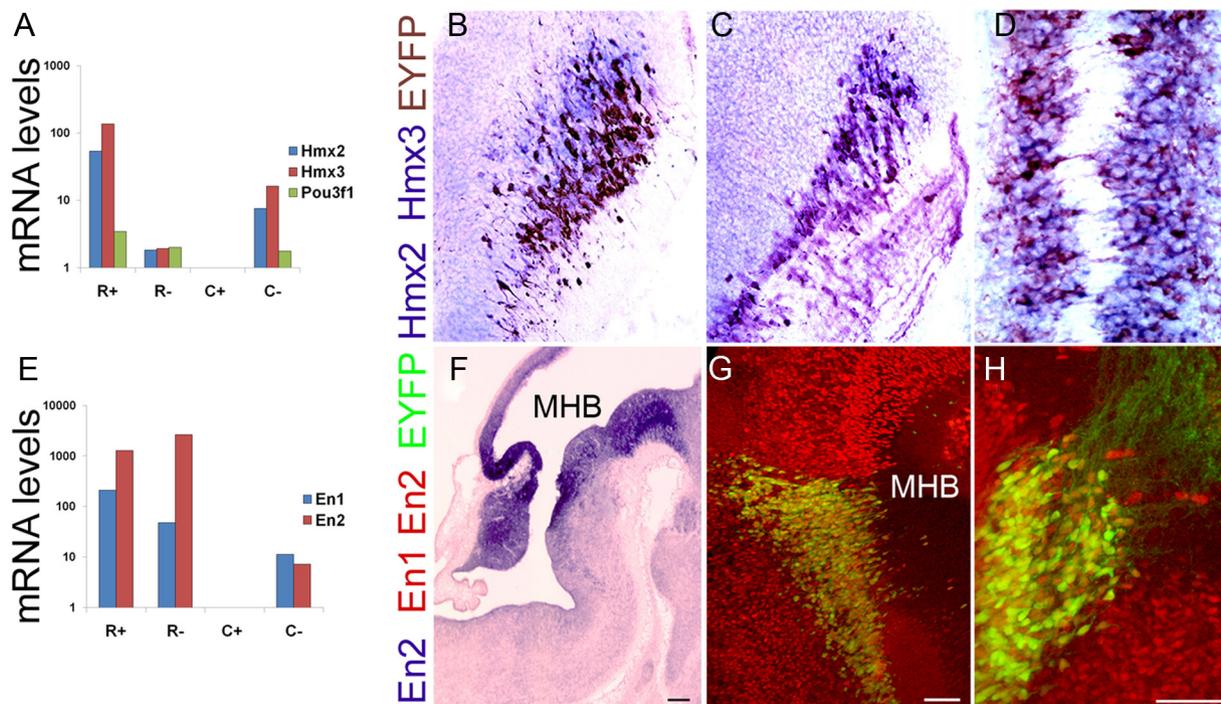
Figure 5. Verification of rostral 5HT neuron-enriched HD gene expression. **A**, Taqman RT-PCR confirmed enriched expression of Hmx2, Hmx3, and Pou3f1 homeodomain genes in rostral (R$^+$) but not caudal (C$^+$) 5HT neurons. **B–D**, Double-label *in situ* hybridization (blue) and immunohistochemistry for EYFP (brown) confirmed expression of Hmx2 (**B**) and Hmx3 (**C**) in E12.5 rostral 5HT neurons. **D**, Hmx2 expression was maintained in rostral 5HT neurons at E16.5. **E**, Taqman RT-PCR verification of enriched En1 and En2 gene expression in E12.5 rostral 5HT neurons (R$^+$) as well as non-5HT cells (R$^-$ and C$^-$) but not caudal 5HT neurons (C$^+$). **F**, *In situ* hybridization for En2 at E12.5 shows a broad domain of expression on either side of the MHB. Immunohistochemical staining with a pan-engrailed antibody (red) detected En1 and En2 proteins in EYFP$^+$ (green) 5HT neurons in rhombomere 1 at E12.5. **G**, En1/2 protein expression persisted in rostral 5HT neurons at E14.5. Scale bars: **B**, **C**, **G**, 50 μm; **D**, **H**, 100 μm; **F**, 500 μm.

circuitry (Rousso et al., 2008). We found a 2.1-fold enrichment of FoxP1 in R$^+$ and C$^+$. Immunohistochemical detection of FoxP1 indicated that FoxP1 protein was expressed by a large number of both rostral and caudal 5HT neurons at E12.5 (Fig. 4 *D–F*). Altogether, the verified highly enriched expression of these genes in R$^+$ and C$^+$ suggests new candidate regulators of 5HT neuron development.

Gene ontology and pathway enrichment in 5HT neurons
The distinct gene expression profiles detected in 5HT neurons versus reference nonserotonergic cell types suggest 5HT neurons may selectively use particular signaling and biological pathways. We used our recently developed parametric approach (Wang et al., 2008) based on mixed linear models to search for enrichment of sets of genes that operate together in a common signaling pathways or are associated with GO categories: molecular function, biological process, and cellular component. We queried gene sets for canonical pathways and gene ontology terms in the MSigDB collection. Because many gene sets were examined, to control for the rate of false-positive findings by chance, we adjusted nominal *p* values using Bonferroni correction. We identified highly significant enrichment of numerous gene sets for canonical pathways and GO categories in R$^+$C$^+$ profiles relative to reference R$^-$C$^-$ profiles (Table 2; see Dataset 3, available at www.jneurosci.org as supplemental material), which suggests that 5HT neurons perform a variety of specialized functions. Enrichment of numerous gene sets associated with peptide processing is consistent with the known peptidergic activity of some 5HT neurons and further reveals the molecules that may be required for use of these peptides as serotonergic signals. A large number of gene sets associated with ion transport and G-protein-coupled

receptor pathways may reflect the complexity of afferent signaling systems regulating 5HT neuron activity and is consistent with the idea that cell surface channels and receptors are a major determinant of cell type heterogeneity in the nervous system (Doyle et al., 2008).

Finally, our analyses identified nine significantly enriched gene sets associated with lipid and specifically sphingolipid (SL) metabolism in R$^+$ and C$^+$ compared to reference groups R$^-$ and C$^-$ (Table 2). SLs have been suggested to influence many aspects of nervous system development including neuronal proliferation, differentiation and axonal growth, and synaptic vesicle exocytosis (Colombaioni and Garcia-Gil, 2004; Darios et al., 2009). Ceramide has been shown to promote axonal growth and branching in cultured hippocampal neurons (Schwarz and Futerman, 1997). We speculate that serotonergic enrichment of SL metabolic pathways during the period of 5HT neuron maturation may be required to support the exuberant and complex axonogenesis and collateralization that must occur for proper development of this transmitter system.

Rostral 5HT neuron transcriptome landscape
The segregation of several hundred R$^+$ or C$^+$ expressed genes into four additional clusters (clusters II–IV) suggested previously unrecognized deep molecular heterogeneity in these two groups of embryonic 5HT neurons. We, therefore, examined these clusters individually to identify molecular signatures that distinguish rostral and caudal 5HT neurons.

Cluster II (Table 3) is comprised of 94 probe sets corresponding to 84 unique transcripts enriched in R$^+$ (supplemental Table S9, available at www.jneurosci.org as supplemental material). This list revealed the highly enriched expression of two genes,

Table 4. Top genes with enriched expression in C $^+$ (cluster IV) and C $^+$ C $^-$ (cluster V)

Affy ID	Fold change	Gene symbol	Gene title
C $^+$-enriched genes			
1441429_at	20.3	Irs4	Insulin receptor substrate 4
1442724_at	15.6	Dlk1	δ-like 1 homolog (*Drosophila*)
1455436_at	13.0	Diras2	DIRAS family, GTP-binding RAS-like 2
1418589_a_at	11.9	Mlf1	Myeloid leukemia factor 1
1457733_at	9.7	—	—
1457635_s_at	9.6	Nr3c1	Nuclear receptor subfamily 3, group C, member 1
1424250_a_at	9.3	Arhgef3	Rho guanine nucleotide exchange factor (GEF) 3
1438540_at	8.8	Col25a1	Collagen, type XXV, α 1
1460482_at	7.7	3110047P20Rik	RIKEN cDNA 3110047P20 gene
1449939_s_at	7.4	Dlk1	δ-like 1 homolog (*Drosophila*)
1445268_at	6.1	—	—
1418756_at	5.6	Trh	Thyrotropin-releasing hormone
1456096_at	5.5	6430573F11Rik	RIKEN cDNA 6430573F11 gene
1437868_at	5.3	BC023892	cDNA sequence BC023892
1441258_at	5.2	AF529169	cDNA sequence AF529169
1433787_at	5.2	Nell1	NEL-like 1 (chicken)
1423836_at	5.1	Zfp503	Zinc finger protein 503
1448125_at	5.0	Rit2	Ras-like without CAAX 2
1427122_at	4.9	Copg2as2	Coatomer protein complex, subunit γ 2, antisense 2
1439827_at	4.9	Adamts12	A disintegrin-like and metallopeptidase (reprolysin type) with thrombospondin type 1 motif, 12
1428765_at	4.7	Meg3	Maternally expressed 3
1417217_at	4.6	Magel2	Melanoma antigen, family L, 2
1435513_at	4.4	Htr2c	5-Hydroxytryptamine (serotonin) receptor 2C
1449465_at	4.4	Reln	Reelin
1427123_s_at	4.2	Copg2as2	Coatomer protein complex, subunit γ 2, antisense 2
C $^+$ C $^-$-enriched genes			
1418415_at	68.0	Hoxb5	Homeobox B5
1441070_at, 1429019_s_at	46.0, 5.5	Hoxb3	Homeobox B3
1458622_at, 1455426_at	39.7, 4.7	Hoxa5	Homeobox A5
1423756_s_at	33.8	Hoxc4	Homeobox C4
1449368_at, 1421841_at	23.1, 7.2	Hoxd3	Homeobox D3
1428429_at, 1452421_at	19.7, 4.2	Hoxa3	Homeobox A3
1451277_at	17.6	Hoxc5	Homeobox C5
1439885_at	16.9	Hoxb6	Homeobox B6
1457966_at	12.5	Hoxb4	Homeobox B4
1438042_at	10.9	AI448005	Expressed sequence AI448005
1444543_at	10.1	—	—
1440177_at, 1434818_at, 1455299_at	9.8, 8.8, 6.9	Ttr	Transthyretin
1460379_at	8.4	Hoxb2	Homeobox B2
1428026_at	8.1	Hoxa4	Homeobox A4
1416783_at	7.7	Tac1	Tachykinin 1
1460214_at	7.6	Dcn	Decorin
1450209_at	6.9	Shox2	Short stature homeobox 2
1420401_a_at	6.9	Hoxa2	Homeobox A2
1456229_at	5.7	0610040B09Rik	RIKEN cDNA 0610040B09 gene
1458470_at	5.4	A930038C07Rik	RIKEN cDNA A930038C07 gene
1416561_at	4.9	Gad1	Glutamic acid decarboxylase 1
1430596_s_at	4.9	Sorl1	Sortilin-related receptor, LDLR class A repeats-containing
1460693_a_at	4.2	Hoxb7/Hoxb8	Homeobox B7/homeobox B8
1451761_at	3.9	—	—
1451461_a_at	3.9	—	—

Hmx2 (Nkx5.2) and Hmx3 (Nkx5.1), encoding related homeodomain proteins in R $^+$ with little or no expression detected in C $^+$. Taqman RT-PCR confirmed the enriched expression of both Hmx2 (80-fold) and Hmx3 (120-fold) in R $^+$ (Fig. 5A). *In situ* hybridization double-label immunohistochemistry at E12.5 demonstrated that Hmx2 (Fig. 5B) marked all rostral 5HT neurons, while Hmx3 expression was observed in a subpopulation of rostral 5HT neurons (Fig. 5C). Hmx2 expression was maintained at E16.5 (Fig. 5D), while Hmx3 transcript was detectable at a lower level at E14.5 (data not shown). The expression of these genes provides a molecular signature of serotonergic neurons in

the rostral hindbrain. Verification of Pou3f1, a POU homeodomain transcription factor, indicated enriched expression to a lesser extent than the Hmx genes in R $^+$ (Fig. 5A).

Cluster III comprises 27 probe sets that correspond to 25 unique transcripts enriched in both R $^+$ and R $^-$ cells (Table 3; supplemental Table S10, available at www.jneurosci.org as supplemental material). Of particular interest in this list are the engrailed homeodomain transcription factor genes, En1 and En2, which have been extensively studied for their multiple roles in nervous system development including establishment of the midbrain-hindbrain boundary, cerebellum development, axonal

guidance, and dopamine neuron development and survival (Joyner, 1996; Simon et al., 2004). Taqman RT-PCR confirmed their enrichment in R^+ as well as R^- and C^- reference cell populations but not C^+ (Fig. 5E). *In situ* hybridization for En2 at E12.5 showed a broad domain of expression that spanned both sides of the mid-hindbrain boundary (MHB) (Fig. 5F). Postmitotic rostral 5HT neurons have migrated from the ventricular zone by E12.5 and were situated in the En2+ region below the MHB. Immunohistochemical detection with a pan-engrailed antibody (Davis et al., 1991) showed strong and persistent expression of En1/En2 proteins in a subset of postmitotic rostral 5HT neurons in rhombomere 1 (r1) at least through E14.5 (Fig. 5G,H). These findings raise the possibility that engrailed genes play cell-autonomous roles in the differentiation and maintenance of rostral 5HT neurons.

Caudal 5HT neuron transcriptome landscape

We next examined clusters IV and V to identify transcripts enriched in caudal 5HT neurons. Cluster IV comprises 300 probe sets, which correspond to 270 unique transcripts and 29 RIKEN cDNAs enriched in C^+ neurons (Table 4; supplemental Table S11, available at www.jneurosci.org as supplemental material). We identified several imprinted genes, Dlk1, Meg3, Magel2, and Copg2as2, each with severalfold-enriched expression in C^+. However, unlike the Hmx and En genes, whose expression was overwhelmingly enriched in rostral 5HT neurons, these C^+-enriched genes also showed significant but less enrichment in R^+ cells (Dataset 2, available at www.jneurosci.org as supplemental material). These genes are members of three distinct imprinted domains present on different chromosome and thus raise the possibility that stringent regulation of gene dosage is important for proper 5HT neuron development and function. Further examination of our databases revealed an additional 70 probe sets corresponding to 43 unique imprinted genes showing expression in rostral and caudal 5HT neurons (supplemental Table S12, available at www.jneurosci.org as supplemental material). Only three of these, Ancient, Magel2, Ddc, are reported in the Allen Brain Library list of genes with a TPH2-like expression pattern in the adult mouse brain.

Cluster V represents an additional group of serotonergic genes whose expression was enriched in both C^+ and C^- cells. This cluster comprises 146 probe sets, which corresponds to 113 unique genes and 9 RIKEN cDNAs (Table 4; supplemental Table S13, available at www.jneurosci.org as supplemental material). A striking feature of this profile is the numerous Hox paralogues whose expression was enriched in C^+ and C^- up to 70-fold relative to R^+ and R^-. Our array studies detected highly enriched expression of 14 Hox genes and their cofactors Meis1 and Meis 2 in C^+, whereas there was little or no expression of these Hox genes in R^+ (Dataset 2, available at www.jneurosci.org as supple-
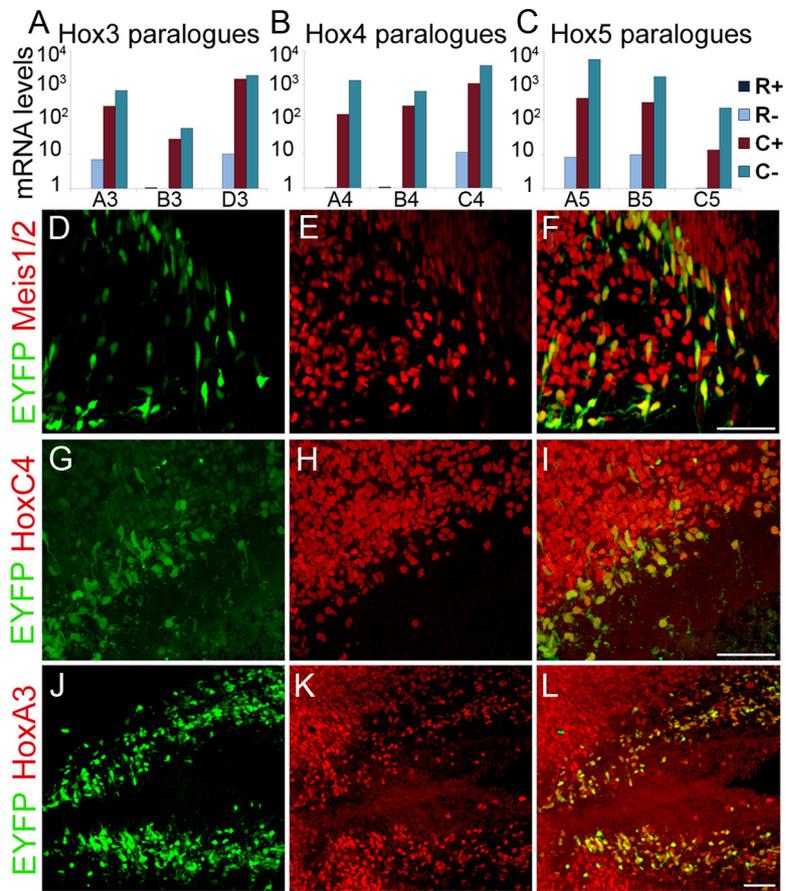
Figure 6. Verification of Hox gene expression in caudal 5HT neurons. ***A–C***, Taqman RT-PCR confirmed the expression of Hox3 (***A***), Hox4 (***B***), and Hox5 (***C***) paralogues in caudal (C^+) but not rostral (R^+) 5HT neurons. ***D–L***, Immunohistochemical staining for the Hox cofactors, Meis 1 and Meis 2, and Hox proteins. ***D–F***, Meis1 and Meis2 (***E***) were detected in caudal 5HT neurons (***D***) with a pan-anti-Meis antibody (***F***, overlay). ***G–I***, HoxC4 protein (***H***) was detected in caudal 5HT neurons (***G***, ***I***, overlay). ***J–L***, HoxA3 protein (***K***) was detected in most caudal 5HT neurons (***J***) at E12.5 (***L***, overlay). Scale bars: ***D–L***, 50 μm.

mental material). Hox genes are well known for their early roles in patterning morphological identities of embryonic structures along the anterior–posterior body axis (Pearson et al., 2005), and more recently they have been implicated in repression of serotonergic fate in rhombomere 4 (Pattyn et al., 2003) and specifying spinal motor-neuron pool identity (Dasen et al., 2005). We verified enrichment of Hox3, Hox4, and Hox5 paralogues by Taqman RT-PCR (Fig. 6A–C). Expression of Meis1 and Meis2 (Fig. 6D–F), HoxC4 (Fig. 6G–I), and HoxA3 (Fig. 6J–L) proteins was confirmed by immunohistochemistry in caudal 5HT neurons. At E12.5, Meis1/2 and HoxA3 expression spanned the caudal hindbrain and marked most caudal 5HT neurons. HoxC4 expression extended from the spinal cord and into the most posterior hindbrain thus marking only subset of caudal 5HT neurons. The expression of Hox genes was also reported in array studies of differentiated 5HT neurons derived from a rhesus monkey embryonic stem cell line (Bethea et al., 2009). Together, these findings suggest Hox proteins and their cofactors play important roles in the maturation of postmitotic caudal 5HT neurons.

Gene ontology and differential pathway enrichment in rostral and caudal 5HT neurons

We compared gene set enrichment in R^+ versus C^+ expression profiles to further explore the potential functional and metabolic differences between rostral and caudal 5HT neurons. Numerous

Table 5. Gene ontology and pathway enrichment in R$^+$ versus C$^+$ 5HT neurons

Code	Gene set name	Size	Bon
R$^+$ molecular function-enriched gene sets			
346	Substrate-specific transmembrane transporter activity	152/308	0.02889313
271	Protein kinase activity	129/264	0.00560058
347	Substrate-specific transporter activity	167/347	0.00245254
163	Kinase activity	156/342	0.00065897
328	Small GTPase regulator activity	21/64	0.00779472
C$^+$ biological process-enriched gene sets			
62	Calcium ion transport	15/24	0.00074155
168	Di-, trivalent inorganic cation transport	18/29	0.00021683
800	Transport	392/703	0.00019125
246	G-protein-coupled receptor protein signaling pathway	114/290	3.6497×10^{-5}
C$^+$ molecular function-enriched gene sets			
18	Aminopeptidase activity	8/10	0.00490194
174	Lipid kinase activity	8/11	0.03140293
38	Calcium channel activity	19/30	0.01250318
118	GTPase regulator activity	77/122	0.00713664
279	Protein serine threonine kinase activity	116/189	2.405×10^{-5}
168	Ligand-gated channel activity	17/32	0.00144691
384	Transmembrane transporter activity	174/338	0.01154298
188	Metal ion transmembrane transporter activity	66/131	0.00658676

Bon, Bonferroni-corrected p value.

gene sets were differentially enriched in R$^+$ and C$^+$ neurons, including those associated with intracellular signaling pathways, GPCR pathways, channel activity, integrin pathways, axon guidance, and ion transport. Gene sets associated with several metabolic pathways were also differentially enriched in either R$^+$ or C$^+$, thus further indicating major differences in R$^+$ and C$^+$ gene expression and further supporting possibility of significant physiological differences in these serotonergic cell types (Table 5, see Dataset 4, available at www.jneurosci.org as supplemental material for complete list).

Discussion

This study reports the isolation of postmitotic 5HT neurons from the embryonic mouse hindbrain by flow cytometry and the use of these cells to profile 5HT neuron gene expression. Our array studies detected expression of ~9000 unique gene products in E12.5 5HT neurons with enriched expression of nearly 800 of these genes. The number of unique genes we detected as expressed in 5HT neurons corresponds strikingly well to the ~10,000 unique genes that are expressed in a single *Aplysia* 5HT interneuron. Few of the most highly enriched 5HT expressed genes, however, were common to these two kinds of 5HT neurons (Moroz et al., 2006). We identified 250 genes whose expression was comparably enriched in both rostral and caudal 5HT neurons and therefore these genes represent potential new markers of developing 5HT neurons. Several of these genes encode proteins with well defined functions in other neural and nonneural cell types. We also detected enriched expression of noncoding RNAs and genes encoding potential proteins whose functions are not predictable from primary structure. Furthermore, gene set enrichment analysis identified potential signaling and biological pathways in 5HT neurons that may support specialized functional roles of these cells. Our findings provide an unprecedented knowledge of the expressed genetic architecture of 5HT neurons and continued verification will sharpen our understanding of this architecture.

5HT neurons are anatomically and functionally heterogeneous but the molecular mechanisms that determine these distinctions are obscure because of a lack of comprehensive expression profiling of these cells. Our findings demonstrate deep molecular and biological pathway distinctions between neurons that give rise to the ascending and descending serotonergic subsystems. Previous immunohistochemical studies have reported the differential expression of a small number of genes encoding various neuropeptides, receptors and the transmitters GABA and glutamate in adult 5HT neurons (Chan-Palay et al., 1978; Hökfelt et al., 1978, 2000; Belin et al., 1983; Day et al., 2004; Lacoste et al., 2006). The Allen Institute identified 248 genes with a Tph2-like expression pattern in adults, but it is not known whether these genes are differentially expressed in developing rostral and caudal 5HT neurons. Here we demonstrate the power of whole-genome profiling of purified embryonic 5HT neurons by identifying ~500 genes with major expression differences between developing rostral and caudal 5HT neurons. Many of these genes encode various types of transcription factors, although we also detected differential expression of genes encoding ion channels, intracellular signaling factors, and axonal guidance cues. Rostral and caudal 5HT neurons also display differential enrichment of gene sets that suggest different biological pathways operate in these two anatomically defined populations of 5HT neurons. These findings substantiate the concept derived from genetic fate mapping of 5HT progenitors (Jensen et al., 2008) that despite their common neurotransmitter character distinct developmental programs generate 5HT neurons in the rostral and caudal hindbrain.

The differential expression of numerous homeodomain (HD) genes, including En1, En2, Hmx2, and Hmx3 in rostral 5HT neurons and several Hox in caudal 5HT neurons raises the possibility that different intrinsic transcriptional cascades comprising different HDs may operate in developing postmitotic 5HT neurons. Hmx2 and Hmx3 are required for inner ear development and differentiation of specific hypothalamic neuronal cell types (Wang et al., 2004) but they have not been investigated for a role in 5HT neuron development. En1, 2 are required in a redundant manner for 5HT neuron development (Simon et al., 2005). As En expression was reported to be undetected in 5HT neurons these findings were interpreted as indicating a cell nonautonomous role for En1, 2 in 5HT neuron development. However, more recent intersectional/subtractive genetic cell fate

mapping studies have demonstrated that a pool of En[+] progenitors in r1 give rise to all 5HT neurons that populate the adult B4, B6, and B7 raphe nuclei as well as some 5HT neurons in the B5 and B8 median raphe and B9 nuclei (Jensen et al., 2008). In addition, our array, RT-qPCR and immunohistochemical verification findings presented here indicated highly enriched expression of En1 and En2 in an anterior subset of postmitotic rostral 5HT neurons in r1. Together, these findings strongly suggest that rather than playing a cell nonautonomous role, En1/2 genes have intrinsic roles in rostral 5HT neurons.

Our array and verification studies showed highly enriched expression of Hmx2 and Hmx3 in rostral 5HT neurons with no detectable expression of these genes in caudal 5HT neurons. Furthermore, Hox expression was detected in caudal 5HT neurons but not in rostral ones. Thus, rostral 5HT neurons can be defined as an Hmx[+] subtype and caudal 5HT neurons as a Hox[+] subtype. Our findings also define two rostral postmitotic 5HT neuron subtypes (Hmx[+]En[+] and Hmx[+]En[−]) based on the differential expression of En1/2 hence corroborating evidence (Jensen et al., 2008) for serotonergic heterogeneity even greater than suggested by simple rostral and caudal anatomical distinctions. An important question to address experimentally is whether or not En1/2 and the other HD expression constitute an HD code that is required in specific subsets of postmitotic 5HT neurons to direct and maintain heterogeneous programs of serotonergic differentiation, cell body migration, axonal trajectories, or electrophysiological properties.

Our transcriptome studies have identified many previously unrecognized serotonergic genes with potential roles in disease pathogenesis. Of particular interest are the cell adhesion genes, *Cntnap2*, *Nrxn1*, and *Cdh10*, which we have shown here to be expressed in 5HT neurons and whose common and rare genetic variants have been associated with autism susceptibility (Arking et al., 2008; Kim et al., 2008; Wang et al., 2009). These genes can now be investigated to determine what role they play in 5HT neurons and whether their disrupted function results in specific disease endophenotypes. Thus, our databases provide a unique bioinformatics resource to help determine serotonergic expression of genes identified in human psychiatric genome association and linkage studies.

Interestingly, we found expression of 43 different imprinted genes in rostral and caudal 5HT neurons (supplemental Table 12, available at www.jneurosci.org as supplemental material), of which 19 were enriched in 5HT neurons. There are 131 currently known mouse imprinted genes including snoRNAs and miRNAs (http://www.har.mrc.ac.uk/). Many imprinted genes are expressed in the brain and are thought to play critical roles in neurodevelopmental disorders such as autism (Wilkinson et al., 2007). Serotonergic expression of imprinted genes, however, has not been investigated and thus our findings raise the intriguing concept that maternal versus paternal gene expression dosage is important for normal serotonergic function and serotonergic modulation of behavior. An interesting example is Magel2, a paternally imprinted gene that encodes a member of MAGE domain family of proteins (Barker and Salehi, 2002) that is nearly fivefold enriched in C[+]. Magel2 and necdin, another MAGE domain imprinted gene, are located near one another in the chromosomal 15q11–q13 region, which when deleted from the paternal allele results in Prader-Willi syndrome (PWS) and when deleted from the maternal allele results in Angelman syndrome (Horsthemke and Wagstaff, 2008). Among the many behavioral and physiological defects present in children with PWS are severe respiratory abnormalities including frequent apneas and irregu-

lar rhythms (Nixon and Brouillette, 2002). Recent studies in mice have shown that Necdin is also expressed in developing and adult 5HT neurons (Zanella et al., 2008) and as shown here (Dataset 2, available at www.jneurosci.org as supplemental material) at least as early as E12.5. Loss of Necdin function in mice results in defects in 5HT neuron axonal outgrowth and transmitter vesicles (Lee et al., 2005; Zanella et al., 2008). In addition, Necdin^{−/−} mice have respiratory deficits that resemble those in PWS (Ren et al., 2003; Zanella et al., 2008) and is consistent with our finding of severe respiratory deficits in 5HT deficient Pet-1^{−/−} neonates (Erickson et al., 2007). Similarly, Magel2^{−/−} mice have serotonergic deficits (Mercer et al., 2009) and therefore combined loss of function of Necdin and Magel2 in 5HT neurons may contribute to the respiratory deficits seen in PWS. Further support for an important role of Magel2 in 5HT neuron development is the additional behavioral similarities of Pet-1^{−/−} and Magel2^{−/−} mice, including increased anxiety in novel environments and maternal behavior defects (Mercer and Wevrick, 2009; Mercer et al., 2009). The latter abnormality is likely to account for the poor survival of neonates born to Magel2^{−/−} dams and is consistent with recent findings from our laboratory using Pet-1^{−/−} females (Lerch-Haner et al., 2008) and confirmed with TPH2 nulls (Alenina et al., 2009) that brain 5HT is critical for reproductive success. Finally, the PWS imprinted region contains several other imprinted and nonimprinted genes. Examination of our array database indicates serotonergic expression of additional genes in this region including the imprinted genes, MKRN3, SNRF/SNRPN, UBE3a, and the biallelically expressed GABRB3 gene. Together, these findings suggest expression of the 15q11–q13 region may play an important role in 5HT neuron development and its altered dosage in these cells may contribute to neurodevelopmental disorders.

In conclusion, we have identified numerous potential new determinants of 5HT neuron development and function including several homeodomain-encoding genes whose differential expression offers a molecular classification of 5HT neuron subtypes. Our findings provide a wealth of new knowledge and experimentally testable hypotheses about the genetic networks that generate serotonin neuron subtypes and the potential roles of serotonergic genes in disease pathogenesis.

References

Alenina N, Kikic D, Todiras M, Mosienko V, Qadri F, Plehm R, Boyé P, Vilianovitch L, Sohr R, Tenner K, Hörtnagl H, Bader M (2009) Growth retardation and altered autonomic control in mice lacking brain serotonin. Proc Natl Acad Sci U S A 106:10332–10337.

Ansorge MS, Hen R, Gingrich JA (2007) Neurodevelopmental origins of depressive disorders. Curr Opin Pharmacol 7:8–17.

Arking DE, Cutler DJ, Brune CW, Teslovich TM, West K, Ikeda M, Rea A, Guy M, Lin S, Cook EH, Chakravarti A (2008) A common genetic variant in the neurexin superfamily member CNTNAP2 increases familial risk of autism. Am J Hum Genet 82:160–164.

Barker PA, Salehi A (2002) The MAGE proteins: emerging roles in cell cycle progression, apoptosis, and neurogenetic disease. J Neurosci Res 67:705–712.

Beck SG, Pan YZ, Akanwa AC, Kirby LG (2004) Median and dorsal raphe neurons are not electrophysiologically identical. J Neurophysiol 91:994–1005.

Belin MF, Nanopoulos D, Didier M, Aguera M, Steinbusch H, Verhofstad A, Maitre M, Pujol JF (1983) Immunohistochemical evidence for the presence of gamma-aminobutyric acid and serotonin in one nerve cell. A study on the raphe nuclei of the rat using antibodies to glutamate decarboxylase and serotonin. Brain Res 275:329–339.

Benjamini Y, Hochberg Y (1995) Controlling the false discovery rate: a practical and powerful approach to multiple testing. J R Stat Soc 57:289–300.

Bethea CL, Reddy AP, Pedersen D, Tokuyama Y (2009) Expression profile of differentiating serotonin neurons derived from rhesus embryonic stem cells and comparison to adult serotonin neurons. Gene Expr Patterns 9:94–108.

Cahoy JD, Emery B, Kaushal A, Foo LC, Zamanian JL, Christopherson KS, Xing Y, Lubischer JL, Krieg PA, Krupenko SA, Thompson WJ, Barres BA (2008) A transcriptome database for astrocytes, neurons, and oligodendrocytes: a new resource for understanding brain development and function. J Neurosci 28:264–278.

Chan-Palay V, Jonsson G, Palay SL (1978) Serotonin and substance P coexist in neurons of the rat's central nervous system. Proc Natl Acad Sci U S A 75:1582–1586.

Cho G, Lim Y, Zand D, Golden JA (2008a) Sizn1 is a novel protein that functions as a transcriptional coactivator of bone morphogenic protein signaling. Mol Cell Biol 28:1565–1572.

Cho G, Bhat SS, Gao J, Collins JS, Rogers RC, Simensen RJ, Schwartz CE, Golden JA, Srivastava AK (2008b) Evidence that SIZN1 is a candidate X-linked mental retardation gene. Am J Med Genet A 146A:2644–2650.

Colombaioni L, Garcia-Gil M (2004) Sphingolipid metabolites in neural signalling and function. Brain Res Brain Res Rev 46:328–355.

Darios F, Wasser C, Shakirzyanova A, Giniatullin A, Goodman K, Munoz-Bravo JL, Raingo J, Jorgacevski J, Kreft M, Zorec R, Rosa JM, Gandia L, Gutiérrez LM, Binz T, Giniatullin R, Kavalali ET, Davletov B (2009) Sphingosine facilitates SNARE complex assembly and activates synaptic vesicle exocytosis. Neuron 62:683–694.

Dasen JS, Tice BC, Brenner-Morton S, Jessell TM (2005) A Hox regulatory network establishes motor neuron pool identity and target-muscle connectivity. Cell 123:477–491.

Davis CA, Holmyard DP, Millen KJ, Joyner AL (1991) Examining pattern formation in mouse, chicken and frog embryos with an En-specific antiserum. Development 111:287–298.

Day HE, Greenwood BN, Hammack SE, Watkins LR, Fleshner M, Maier SF, Campeau S (2004) Differential expression of 5HT-1A, alpha 1b adrenergic, CRF-R1, and CRF-R2 receptor mRNA in serotonergic, gamma-aminobutyric acidergic, and catecholaminergic cells of the rat dorsal raphe nucleus. J Comp Neurol 474:364–378.

Doyle JP, Dougherty JD, Heiman M, Schmidt EF, Stevens TR, Ma G, Bupp S, Shrestha P, Shah RD, Doughty ML, Gong S, Greengard P, Heintz N (2008) Application of a translational profiling approach for the comparative analysis of CNS cell types. Cell 135:749–762.

Eisen MB, Spellman PT, Brown PO, Botstein D (1998) Cluster analysis and display of genome-wide expression patterns. Proc Natl Acad Sci U S A 95:14863–14868.

Erickson JT, Shafer G, Rossetti MD, Wilson CG, Deneris ES (2007) Arrest of 5HT neuron differentiation delays respiratory maturation and impairs neonatal homeostatic responses to environmental challenges. Respir Physiol Neurobiol 159:85–101.

Gargaglioni LH, Bícegoa KC, Branco LG (2008) Brain monoaminergic neurons and ventilatory control in vertebrates. Respir Physiol Neurobiol 164:112–122.

Hendricks T, Francis N, Fyodorov D, Deneris ES (1999) The ETS domain factor Pet-1 is an early and precise marker of central 5-HT neurons and interacts with a conserved element in serotonergic genes. J Neurosci 19:10348–10356.

Hendricks TJ, Fyodorov DV, Wegman LJ, Lelutiu NB, Pehek EA, Yamamoto B, Silver J, Weeber EJ, Sweatt JD, Deneris ES (2003) Pet-1 ETS gene plays a critical role in 5-HT neuron development and is required for normal anxiety-like and aggressive behavior. Neuron 37:233–247.

Hodges MR, Tattersall GJ, Harris MB, McEvoy SD, Richerson DN, Deneris ES, Johnson RL, Chen ZF, Richerson GB (2008) Defects in breathing and thermoregulation in mice with near-complete absence of central serotonin neurons. J Neurosci 28:2495–2505.

Hökfelt T, Ljungdahl A, Steinbusch H, Verhofstad A, Nilsson G, Brodin E, Pernow B, Goldstein M (1978) Immunohistochemical evidence of substance P-like immunoreactivity in some 5-hydroxytryptamine-containing neurons in the rat central nervous system. Neuroscience 3:517–538.

Hökfelt T, Arvidsson U, Cullheim S, Millhorn D, Nicholas AP, Pieribone V, Seroogy K, Ulfhake B (2000) Multiple messengers in descending serotonin neurons: localization and functional implications. J Chem Neuroanat 18:75–86.

Holmes A (2008) Genetic variation in cortico-amygdala serotonin function and risk for stress-related disease. Neurosci Biobehav Rev 32:1293–1314.

Horsthemke B, Wagstaff J (2008) Mechanisms of imprinting of the Prader-Willi/Angelman region. Am J Med Genet A 146A:2041–2052.

Jacob J, Ferri AL, Milton C, Prin F, Pla P, Lin W, Gavalas A, Ang SL, Briscoe J (2007) Transcriptional repression coordinates the temporal switch from motor to serotonergic neurogenesis. Nat Neurosci 10:1433–1439.

Jensen P, Farago AF, Awatramani RB, Scott MM, Deneris ES, Dymecki SM (2008) Redefining the serotonergic system by genetic lineage. Nat Neurosci 11:417–419.

Joyner AL (1996) Engrailed, Wnt and Pax genes regulate midbrain–hindbrain development. Trends Genet 12:15–20.

Kim HG, Kishikawa S, Higgins AW, Seong IS, Donovan DJ, Shen Y, Lally E, Weiss LA, Najm J, Kutsche K, Descartes M, Holt L, Braddock S, Troxell R, Kaplan L, Volkmar F, Klin A, Tsatsanis K, Harris DJ, Noens I, et al. (2008) Disruption of neurexin 1 associated with autism spectrum disorder. Am J Hum Genet 82:199–207.

Kimura T, Arakawa Y, Inoue S, Fukushima Y, Kondo I, Koyama K, Hosoi T, Orimo A, Muramatsu M, Nakamura Y, Abe T, Inazawa J (1997) The brain finger protein gene (ZNF179), a member of the RING finger family, maps within the Smith-Magenis syndrome region at 17p11.2. Am J Med Genet 69:320–324.

Kocsis B, Varga V, Dahan L, Sik A (2006) Serotonergic neuron diversity: identification of raphe neurons with discharges time-locked to the hippocampal theta rhythm. Proc Natl Acad Sci U S A 103:1059–1064.

Lacoste B, Riad M, Descarries L (2006) Immunocytochemical evidence for the existence of substance P receptor (NK1) in serotonin neurons of rat and mouse dorsal raphe nucleus. Eur J Neurosci 23:2947–2958.

Lee S, Walker CL, Karten B, Kuny SL, Tennese AA, O'Neill MA, Wevrick R (2005) Essential role for the Prader-Willi syndrome protein necdin in axonal outgrowth. Hum Mol Genet 14:627–637.

Le François B, Czesak M, Steubl D, Albert PR (2008) Transcriptional regulation at a HTR1A polymorphism associated with mental illness. Neuropharmacology 55:977–985.

Leonardo ED, Hen R (2006) Genetics of affective and anxiety disorders. Annu Rev Psychol 57:117–137.

Lerch-Haner JK, Frierson D, Crawford LK, Beck SG, Deneris ES (2008) Serotonergic transcriptional programming determines maternal behavior and offspring survival. Nat Neurosci 11:1001–1003.

Lillesaar C, Tannhäuser B, Stigloher C, Kremmer E, Bally-Cuif L (2007) The serotonergic phenotype is acquired by converging genetic mechanisms within the zebrafish central nervous system. Dev Dyn 236:1072–1084.

Lucki I (1998) The spectrum of behaviors influenced by serotonin. Biol Psychiatry 44:151–162.

Mason P (2001) Contributions of the medullary raphe and ventromedial reticular region to pain modulation and other homeostatic functions. Annu Rev Neurosci 24:737–777.

Mercer RE, Wevrick R (2009) Loss of magel2, a candidate gene for features of Prader-Willi syndrome, impairs reproductive function in mice. PLoS ONE 4:e4291.

Mercer RE, Kwolek EM, Bischof JM, van Eede M, Henkelman RM, Wevrick R (2009) Regionally reduced brain volume, altered serotonin neurochemistry, and abnormal behavior in mice null for the circadian rhythm output gene Magel2. Am J Med Genet B Neuropsychiatr Genet 150B:1085–1099.

Moroz LL, Edwards JR, Puthanveettil SV, Kohn AB, Ha T, Heyland A, Knudsen B, Sahni A, Yu F, Liu L, Jezzini S, Lovell P, Iannucculli W, Chen M, Nguyen T, Sheng H, Shaw R, Kalachikov S, Panchin YV, Farmerie W, et al. (2006) Neuronal transcriptome of *Aplysia*: neuronal compartments and circuitry. Cell 127:1453–1467.

Mühlfriedel S, Kirsch F, Gruss P, Chowdhury K, Stoykova A (2007) Novel genes differentially expressed in cortical regions during late neurogenesis. Eur J Neurosci 26:33–50.

Ng L, Bernard A, Lau C, Overly CC, Dong HW, Kuan C, Pathak S, Sunkin SM, Dang C, Bohland JW, Bokil H, Mitra PP, Puelles L, Hohmann J, Anderson DJ, Lein ES, Jones AR, Hawrylycz M (2009) An anatomic gene expression atlas of the adult mouse brain. Nat Neurosci 12:356–362.

Nixon GM, Brouillette RT (2002) Sleep and breathing in Prader-Willi syndrome. Pediatr Pulmonol 34:209–217.

Pattyn A, Vallstedt A, Dias JM, Samad OA, Krumlauf R, Rijli FM, Brunet JF, Ericson J (2003) Coordinated temporal and spatial control of motor neuron and serotonergic neuron generation from a common pool of CNS progenitors. Genes Dev 17:729–737.

Pearson JC, Lemons D, McGinnis W (2005) Modulating Hox gene functions during animal body patterning. Nat Rev Genet 6:893–904.

Potocki L, Bi W, Treadwell-Deering D, Carvalho CM, Eifert A, Friedman EM, Glaze D, Krull K, Lee JA, Lewis RA, Mendoza-Londono R, Robbins-Furman P, Shaw C, Shi X, Weissenberger G, Withers M, Yatsenko SA, Zackai EH, Stankiewicz P, Lupski JR (2007) Characterization of Potocki-Lupski syndrome (dup(17)(p11.2p11.2)) and delineation of a dosage-sensitive critical interval that can convey an autism phenotype. Am J Hum Genet 80:633–649.

Prasad HC, Zhu CB, McCauley JL, Samuvel DJ, Ramamoorthy S, Shelton RC, Hewlett WA, Sutcliffe JS, Blakely RD (2005) Human serotonin transporter variants display altered sensitivity to protein kinase G and p38 mitogen-activated protein kinase. Proc Natl Acad Sci U S A 102: 11545–11550.

Reimers M, Carey VJ (2006) Bioconductor: an open source framework for bioinformatics and computational biology. Methods Enzymol 411:119–134.

Ren J, Lee S, Pagliardini S, Gérard M, Stewart CL, Greer JJ, Wevrick R (2003) Absence of Ndn, encoding the Prader-Willi syndrome-deleted gene necdin, results in congenital deficiency of central respiratory drive in neonatal mice. J Neurosci 23:1569–1573.

Rousso DL, Gaber ZB, Wellik D, Morrisey EE, Novitch BG (2008) Coordinated actions of the forkhead protein Foxp1 and Hox proteins in the columnar organization of spinal motor neurons. Neuron 59:226–240.

Schwarz A, Futerman AH (1997) Distinct roles for ceramide and glucosylceramide at different stages of neuronal growth. J Neurosci 17:2929–2938.

Scott MM, Wylie CJ, Lerch JK, Murphy R, Lobur K, Herlitze S, Jiang W, Conlon RA, Strowbridge BW, Deneris ES (2005) A genetic approach to access serotonin neurons for in vivo and in vitro studies. Proc Natl Acad Sci U S A 102:16472–16477.

Seki N, Hattori A, Muramatsu M, Saito T (1999) cDNA cloning of a human brain finger protein, BFP/ZNF179, a member of the RING finger protein family. DNA Res 6:353–356.

Simon HH, Thuret S, Alberi L (2004) Midbrain dopaminergic neurons: control of their cell fate by the engrailed transcription factors. Cell Tissue Res 318:53–61.

Simon HH, Scholz C, O'Leary DD (2005) Engrailed genes control development of serotonergic and noradrenergic neurons in mid- and hindbrain in a gene dose-dependent manner. Mol Cell Neurosci 28:96–105.

Smyth GK (2005) Limma: linear models for microarray data. Bioinformatics and computational biology solutions using R and Bioconductor (Gentleman R, Carey V, Dudoit S, Irizarry R, Huber W, eds), pp 397–420. New York: Springer.

Sodhi MS, Sanders-Bush E (2004) Serotonin and brain development. Int Rev Neurobiol 59:111–174.

Sugino K, Hempel CM, Miller MN, Hattox AM, Shapiro P, Wu C, Huang ZJ, Nelson SB (2006) Molecular taxonomy of major neuronal classes in the adult mouse forebrain. Nat Neurosci 9:99–107.

Wang K, Zhang H, Ma D, Bucan M, Glessner JT, Abrahams BS, Salyakina D, Imielinski M, Bradfield JP, Sleiman PM, Kim CE, Hou C, Frackelton E, Chiavacci R, Takahashi N, Sakurai T, Rappaport E, Lajonchere CM, Munson J, Estes A, et al. (2009) Common genetic variants on 5p14.1 associate with autism spectrum disorders. Nature 459:528–533.

Wang L, Zhang B, Wolfinger RD, Chen X (2008) An integrated approach for the analysis of biological pathways using mixed models. PLoS Genet 4:e1000115.

Wang W, Grimmer JF, Van De Water TR, Lufkin T (2004) Hmx2 and Hmx3 homeobox genes direct development of the murine inner ear and hypothalamus and can be functionally replaced by *Drosophila* Hmx. Dev Cell 7:439–453.

Wilkinson LS, Davies W, Isles AR (2007) Genomic imprinting effects on brain development and function. Nat Rev Neurosci 8:832–843.

Ye W, Shimamura K, Rubenstein JLR, Hynes MA, Rosenthal A (1998) FGF and Shh signals control dopaminergic and serotonergic cell fate in the anterior neural plate. Cell 93:755–766.

Zanella S, Watrin F, Mebarek S, Marly F, Roussel M, Gire C, Diene G, Tauber M, Muscatelli F, Hilaire G (2008) Necdin plays a role in the serotonergic modulation of the mouse respiratory network: implication for Prader-Willi syndrome. J Neurosci 28:1745–1755.

Zhao ZQ, Chiechio S, Sun YG, Zhang KH, Zhao CS, Scott M, Johnson RL, Deneris ES, Renner KJ, Gereau RW 4th, Chen ZF (2007) Mice lacking central serotonergic neurons show enhanced inflammatory pain and an impaired analgesic response to antidepressant drugs. J Neurosci 27:6045–6053.